Research Paper

The enhanced antitumor-specific immune response with mannose- and CpG-ODN-coated liposomes delivering TRP2 peptide

Chunhui Lai[1,*], Siliang Duan[1,*], Fang Ye[1,2*], Xiaoqiong Hou[1,2], Xi Li[1], Jin Zhao[1], Xia Yu[1], Zixi Hu[1], Zhuoran Tang[1], Fengzhen Mo[1], Xiaomei Yang[1], Xiaoling Lu[1,2,3✉]

1. International Nanobody Research Center of Guangxi, Guangxi Medical University, Nanning, Guangxi, 530021, China
2. The Department of Immunology, Guangxi Medical University, Nanning, Guangxi, 530021, China
3. College of Stomatology, Guangxi Medical University (GXMUCS), Nanning, Guangxi, 530021, China

* These authors contributed equally to this work.

✉ Corresponding author: Xiaoling Lu, Ph.D., Professor, Intenational Nanobody Research Center of Guangxi, Guangxi Medical University, Nanning, Guangxi, 530021, China. Tel: (86) 771-5317 061; Fax: (86) 771-5317 061. Email: luxiaoling@gxmu.edu.cn

Abstract

Purpose: Dendritic cell (DC)-based cancer vaccines is a newly emerging and potent form of immune therapy. As for any new technology, there are still considerable challenges that need to be addressed. Here, we investigate the antitumor potential of a novel liposomal vaccine, M/CpG-ODN-TRP2-Lipo.

Methods: We developed a vaccination strategy by assembling the DC-targeting mannose and immune adjuvant CpG-ODN on the surface of liposomes, which were loaded with melanoma-specific TRP2$_{180-188}$ peptide as liposomal vaccine. M/CpG-ODN-TRP2-Lipo treatment was used to intendedly induce activation of DCs and antitumor- specific immune response in vivo.

Results: Our results demonstrated in vitro that the prepared liposomal particles were efficiently taken up by DCs. This uptake led to an enhanced activation of DCs, as measured by the upregulation of MHC II, CD80, and CD86. Furthermore, M/CpG-ODN-TRP2-Lipo effectively inhibited the growth of implanted B16 melanoma and prolonged the survival of mice. This therapy significantly reduced the number of myeloid-derived suppressor cells (MDSCs) and regulatory T cells, while simultaneously increasing the number of activated T cells, tumor antigen-specific CD8+ cytotoxic T cells, and interferon-γ-producing cells. At the same time, it was found to suppress tumor angiogenesis and tumor cell proliferation, as well as up-regulate their apoptosis. Interestingly, MyD88-knockout mice had significantly shorter median survival times compared to wild-type mice following the administration of M/CpG-ODN-TRP2-Lipo.

Conclusions: The results suggested that the antitumor activities of the vaccine partially rely on the Myd88 signaling pathway. Interestingly, compared to whole tumor cell lysate-based vaccine, M/CpG-ODN-TRP2-Lipo, tumor specific antigen peptide-based vaccine, improved survival of tumor-bearing mice as well as enhanced their antitumor responses. All in all, we describe a novel vaccine formulation, M/CpG-ODN-TRP2-Lipo, with the aim of improving antitumor responses by alleviating the immunosuppressive environment in tumors.

Key words: immunotherapy, liposome, tumor, dendritic cells-based cancer vaccine, tumor antigen-specific CD8+ T-cells

Introduction

Evading immune destruction is a hallmark of cancer [1] that provides a rational approach for next-generation cancer immunotherapy [2]. Recently, cancer immunotherapy has been proven efficacious for the treatment of multiple solid and hematological cancers [3]. Thus far, cancer immunotherapy is

gaining popularity along with the traditional strategies of surgery, chemotherapy, and radiotherapy. Immunotherapy can be divided into "passive" and "active" approaches. Passive immunotherapeutic approaches include the induction of immune responses through transfer of tumor antigen-targeted monoclonal antibodies or T cells to bypass the activation of endogenous immunity [4]. Active immunotherapy includes immune stimulation using immunological checkpoint inhibitors, cytokines, and cancer vaccines to induce *de novo* cancer-specific immunity [3]. Although each approach is built upon a distinct mechanism, the ultimate goal is to activate tumor-specific cytotoxic T lymphocytes (CTLs) and eradicate tumor cells.

Given their potency as the antigen-presenting cells and their central roles in coordinating both innate and adaptive immunity, dendritic cells (DCs) have become one of the best adjuvant vaccination strategies in cancer therapy [5, 6]. Immature DCs constitutively present self-antigens to T cells and promote the differentiation of Tregs and immune tolerance [7]. In contrast, antigen-loaded mature DCs would differentiate naive CD4+ T cells into helper T cells (Th1, Th2, or Th17), and/or naive CD8+ T cells into CTLs [8-10]. DCs are also effective in triggering humoral immunity. However, the maturation and the antigen-presenting ability of DCs are severely compromised within the tumor immunosuppressive environment [11, 12]. Therefore, effective DC-based vaccines are supposed to elicit CD8+ CTLs that specifically and actively recognize antigen peptide-major histocompatibility complex class I (MHC-I) complexes on tumor cells, and then stimulate the production of tumor-killing molecules, granzyme, and/or perforin, break down the immunosuppressive microenvironment surrounding the tumor, and generate long-lived memory CD8+ T cells to prevent cancer relapse [13, 14].

The development of DC-based vaccines has evolved from *ex vivo* antigen loading to *in vivo* DC targeting, both of which have their pros and cons and are under intensive investigation [15]. To date, the identification of DC-specific receptors has stimulated the development of *in vivo* DC-targeting vaccines. It was reported that mannose modified liposomes specifically target DCs, which express mannose receptors (belonging to the C-type lectin receptor family), thus enhancing DC-mediated antitumor activities [16, 17]. So far, there are many other reported DC-specific receptors, such as CD205 [18, 19], and DC-SIGN [20]. In addition, it was found that the delivery of tumor-specific antigen without proper DC maturation stimuli leads to Treg induction and immune tolerance [21, 22]. Therefore, the

co-administration of DC maturation stimuli is critical for improving the immunotherapeutic effect [19, 23]. CpG oligodeoxynucleotides (CpG-ODNs), short synthetic oligodeoxynucleotides containing optimized unmethylated CpG motifs, have progressed into clinical vaccine trials as adjuvants and immunotherapeutic agents [24]. It was reported that CpG-ODNs are captured by DEC-205, a cell surface receptor, and delivered to the intracellular receptor TLR9 [25]. Subsequently, stimulation of TLR9 activates DCs to express increased levels of co-stimulatory molecules such as CD80 and CD86. This is believed to initiate a cascade of innate and adaptive responses. Moreover, the multi-component nature of a cancer vaccine preferentially calls for an effective delivery system. Liposomes and liposome-derived nanovesicles, which can serve as excellent carriers for tumor antigens and/or immune stimuli, have played important roles in vaccine development. Currently, many liposome complexes are under study in clinical trials to evaluate their effectiveness in treating various types of malignancies [26].

Melanoma, also known as malignant melanoma, is a highly invasive and metastatic disease with an increasing incidence and death rate compared to most other cancers [27]. Because melanoma is not sensitive to radiation therapy, the main initial treatment for melanoma is surgical resection. However, other therapies are required for disease control of metastatic melanomas. The identification of tumor-specific antigens in melanoma has sparked hope in immunotherapy for melanoma treatment [28]. Tyrosinase-related protein-2 (TRP2) is an antigen expressed on human and mouse melanoma cells as well as normal melanocytes. Peptide 180-188, an epitope on the TRP2 protein, is restricted by mouse MHC-I H-2K^b and human leukocyte antigen-A2 [29, 30]. Vaccines targeting TRP2$_{180-188}$ demonstrated bio-activity against melanoma [31, 32].

Based on the rationale that mannose might synergize with lipid-conjugated CpG-ODNs, we developed a vaccination strategy by assembling the DC-targeting mannose and immune adjuvant CpG-ODN on the surface of liposomes, which were loaded with melanoma-specific TRP2$_{180-188}$ peptide, as liposomal vaccine (designated as M/CpG-ODN-TRP2-Lipo). Liposomeal vaccine loaded with Mut1 peptide (a lung carcinoma specific antigen peptide) or B16 whole cell lysates, designated as M/CpG-ODN-Mut1-Lipo or M/CpG-ODN-B16-Lipo, respectively, were developed as control. The functional characteristics of M/CpG-ODN-TRP2-Lipo *in vitro* were examined. We used M/CpG-ODN-TRP2-Lipo treatment to specifically induce activation of DCs. The

in vivo antitumor effects for the B16 melanoma model in C57BL/6 mice and the underlying molecular mechanisms were also explored. Our results emphasized the potency of the liposome-delivered DC-targeting vaccines loaded with tumor-specific antigen peptide in combination with potent immunoadjuvant to induce antitumor immune responses. Also, it may provide an efficient and safe strategy for targeting cell-based vaccines for the treatment of tumors.

Materials and methods

Materials

Palmitic acid, mannosamine, and 1,1'-dicyclohexylcarbodiimide (DCC) were purchased from Aladdin (Shanghai, China). The lipids POPC (1-palmitoyl, 2-oleoyl-sn-glycero-3-phosphocholine), cholesterol, DSPE-PEG$_{2000}$ (1,2-distearoyl-sn-glycero-3-phosphoethanolamine-N-[(polyethylene glycol)-2000]), DSPE-PEG$_{2000}$-maleimide, and didecyldimethylammonium bromide (DDAB) were purchased from Avanti Polar Lipids (Alabaster, AL, USA). The α-tocopherol and β-homocysteine were obtained from Sigma (St. Louis, MO, USA). CpG-ODN1826 (5'-TCC ATGACGTTCCTGACGTT-3') was synthesized by Sangon Biotech (Shanghai, China) and was labeled with fluorescein isothiocyanate (FITC) at the 5' end and modified with a thiol group (-HS) at the 3' end for lipid linking. The H-2K^b-restricted peptides Mut1$_{52-59}$ (FEQNTAQP) and TRP2$_{180-188}$ (SVYDFFVWL) were synthesized by Genscript (Nanjing, China). Antibodies used in this study include: anti-CD11b antibody (conjugated to FITC), anti-Ly6G antibody (conjugated to PE) (Beckman Coulter, Brea, CA, USA), anti-CD3 antibody (conjugated to FITC), anti-CD8 antibody (conjugated to FITC), anti-CD4 antibody (conjugated to FITC), anti-CD25 antibody (conjugated to PE-Cy5.5), anti-FoxP3 antibody (conjugated to PE), FoxP3 staining Buffer Set (eBiosciences, San Diego, CA, USA), TRP2-tetramer and TRP2-tetramer (conjugated to PE) (Kuangbo, Beijing, China), and anti-CD31 antibody (Abcam, Cambridge, MA,USA). The proliferating cell nuclear antigen (PCNA) staining kit was acquired from Boster, Wuhan, China.

Cell lines and animals

The C57BL/6-derived dendritic cell line DC2.4 [33] was purchased from Xiangya School of Medicine (Central South University, Changsha, China). The DC2.4 cells were transfected with pCMV/3' Box_CD206 with lipofectamine 2000 (Life Technologies, Carlsbad, CA, USA) following the manufacturer's protocols. Western blotting was performed to confirm the expression of CD206 in the transiently transfected DC2.4 cells. The C57BL/6-derived B16 melanoma cells were obtained from American Type Culture Collection (Manassas, VA, USA). Both cell types were cultured in RPMI-1640 medium (HyClone, Thermo Fisher Scientific, Waltham, MA, USA) supplemented with 10% fetal bovine serum and 1% streptomycin/penicillin (Life Technologies, Carlsbad, CA, USA) in a 37℃, 5% CO$_2$ incubator.

Wild-type female C57BL/6 (H-2K^b) mice (4–6 weeks of age) were purchased from Vital River (Beijing, China). Female Myd88-knockout C57BL/6 (H-2K^b) mice (4–6 weeks of age) were purchased from the Model Animal Research Center of Nanjing University (Nanjing, China). All mice were housed in a specific pathogen-free facility at room temperature of (22 ± 1) °C on a 12/12-hr light/dark cycle with access to food and water *ad libitum*. All of the animal experiments were approved by the Institutional Animal Care and Use Committee of Guangxi Medical University.

Preparation and characterization of liposome vaccines

The mannose lipid was synthesized from palmitic acid, mannosamine, and DCC at a molar ratio of 1:1:1 in our laboratory and analyzed using Fourier transform infrared spectroscopy (FTIR; VERTEX70, Bruker, Germany) and X-ray diffractometry (XRD; X'Pert PRO, PANalytical, Netherlands). The mannose-coated liposomes were synthesized from POPC, cholesterol, DSPE-PEG2000, DDAB, mannose lipid, and α-tocopherol at a molar ratio of 49.8:40:5:3:2:0.2. A thin lipid film was formed under N$_2$ stream and dried in a vacuum for 2 h in order to remove any residual organic solvent. Then, the obtained lipid film layer was hydrated in Tris-HCl (50 mM, pH 7.0), sonicated for 5 min, loaded onto LipoFast LF-50 (Avestin, Canada), and allowed to pass through a 200 nm polycarbonate membrane 20 times, a 100 nm membrane 20 times, and a 50 nm membrane 21 times to form unilamellar liposomes (M-Lipo). DDAB is a kind of chemical substance with a net positive charge. The supplementation of DDAB into liposomes can raise the positive surface potential to form cationic liposomes, which can reduce the degradation rate of the liposomes in the body and improve the encapsulation efficiency of protein polypeptide. Alpha-tocopherol was employed as an antioxidant substance, which helps to avoid air oxidation in the preparation of liposomes. Alpha-tocopherol does not have an adjuvant effect. To facilitate detection of the liposome uptake by DCs, the liposomes were labeled with DiI stain (Beyotime, Jiangsu, China) according to the manufacturer's instructions.

To conjugate CpG-ODN on the M-Lipo surface, DSPE-PEG$_{2000}$-maleimide was mixed with CpG-ODN at a molar ratio of 5:1 at room temperature for 30 min under N$_2$ stream. β-homocysteine of the same molar concentration as the DSPE-PEG$_{2000}$-maleimide was then added and allowed to interact at room temperature for 30 min. Free CpG-ODN was removed following dialysis using a Slide-A-Lyzer MINI Dialysis Unit (MWCO: 10,000; Thermo Fisher Scientific, Waltham, MA, USA) in HEPES buffer (10 mM, pH 6.5). The resulting DSPE-PEG$_{2000}$-CpG-ODN was added to the M-Lipo and allowed to interact at 55°C for 30 min. CpG-ODN-conjugated M-Lipo (M/CpG-ODN-Lipo) was generated after dialysis to remove un-linked CpG-ODN or other small molecule residues.

To obtain the B16 lysate, B16 cells in the log phase were lysed by repeated freeze-thaw cycles and the total protein concentration was measured according to Bradford assay kit manual (Beyotime). Encapsulation of tumor-specific peptide TRP2, Mut1, or B16 lysate into M/CpG-ODN-Lipo was performed following a film hydration procedure as previously described [34]. The free, non-encapsulated antigen peptides or lysate proteins were measured and removed by dialysis. The encapsulation efficiency (EE) was calculated as $(W_{Total}-W_{Free})/W_{Total} \times 100\%$, where W_{Total} is the total amount of antigen added and W_{Free} is the amount of free, non-encapsulated antigen. The resulting liposomes, M/CpG-ODN-TRP2-Lipo, M/CpG-ODN-Mut1-Lipo, and M/CpG-ODN-B16-Lipo, were diluted in dH$_2$O and analyzed using a Zetasizer (Zetasizer Nano S, Malvern, UK) for particle size, zeta potential, and polydispersity index (PDI), and imaged under transmission electron microscopy (TEM; H-7650, Hitachi, Japan) for exploring the particle morphology and structure.

DC targeting, activation assays and serum stability analysis

To observe DC targeting by liposomes, DC2.4 cells seeded in six-well plates (Corning, Lowell, MA, USA) were added with DiI-labeled liposomes (0.19 µmol) and incubated at 37°C for 2 h. After three washes with phosphate-buffered saline (PBS), the cells were fixed with 4% paraformaldehyde for 30 min and the cell nuclei were stained with 4′, 6-diamidino-2-phenylindole (DAPI; Sigma-Aldrich). The cells were imaged by fluorescence microscopy (Eclipse 80i; Nikon, Tokyo, Japan). To examine the significance of mannose in DC uptake of liposomes, DC2.4 cells were cultured in DMEM medium containing 0.5% mannose (Aladdin) overnight before the liposomes were added. To examine the conjugation of CpG-ODN, liposomes containing FITC-labeled CpG-ODN were used. Untreated DCs served as a blank control.

To assess DC activation in response to liposome treatment, DC2.4 cells were incubated with prepared liposomes at 37°C for 48 h. The surface expression levels of MHC-II, CD86, and CD80 were then examined by flow cytometry (Beckman Coulter, Brea, CA, USA), the data were analyzed using Expo32 ADC software (Epics XL; Beckman Coulter). Untreated DCs served as a blank control. DCs treated with TNF-α (10 ng/mL) served as a positive control. To further evaluate the stability of the M/CpG-ODN-TRP2-Lipo particles in serum, the liposomal particles were mixed with PBS containing 50% fetal bovine serum and incubated at 37°C for up to 10 days. After incubation, the particles were added to pulse the DC2.4 cells. Also, the surface expression levels of CD80 and CD86 on the DC cells were examined by flow cytometry.

In vivo tumor growth and mouse survival

To establish a murine model of melanoma, B16 cells were re-suspended at 3×10^5 cells in 100 µL PBS and injected subcutaneously into the right lower abdomen (100 µL/mouse). The mice were then divided into four groups (n = 8 per group) and administered 100 µL PBS, or 2 µg dose of M/CpG-ODN-Mut1-Lipo, M/CpG-ODN-B16-Lipo, or M/CpG-ODN-TRP2-Lipo respectively on days 6, 9, 12, and 15 after the B16 injection. Tumor length (L) and width (W) were measured every 3 days starting from day 6 after the B16 injection, and volume (V) was calculated using the equation: $V = 0.5 \times L \times W^2$.

Safety studies of M/CpG-ODN-TRP2-Lipo

Safety of M/CpG-ODN-TRP2-Lipo was investigated in C57BL/6 mice following a single 2 µg dose of liposomal particles in 100 µL PBS. Mice treated with PBS served as a negative control (n = 8 per group). All the mice were dissected 7 days after the injection. The harvested tissue specimens were stained with hematoxylin and eosin.

Flow cytometry analysis

On day 17 after the B16 injection, the mice were sacrificed by CO$_2$ euthanasia followed by cervical dislocation. The spleen, tumor, and bone marrow were isolated and prepared into single-cell suspensions. The myeloid-derived suppressor cells (MDSCs) within these samples were examined by staining with fluorophore-conjugated anti-CD11b and anti-Ly6G antibodies; activated T cells by anti-CD3 and anti-CD25 antibodies; and Tregs by anti-CD4, anti-CD25, and anti-FoxP3 antibodies. The TRP2-specific CD8$^+$ CTLs were detected using phycoerythrin-conjugated TRP2-tetramer and anti-CD8 antibody.

ELISPOT assay

To quantify the splenocytes capable of producing interferon-γ, suspensions of splenocyte harvested from each group of mice were seeded in 96-well plates (1×10^5 cells per well) (Dakewe, Shenzhen, China) and stimulated with TRP2 peptide (2 µg/well) at 37°C for 16 h. Then, the IFN-γ positive cells were detected using an ELISPOT assay kit (Dakewe Co., Shenzhen, China), imaged under a CTL Immunospot analyzer (CTL, Shaker Height, OH, USA), and analyzed with Immunospot 5.0 Pro software (CTL).

Immunohistochemistry

The lung, spleen, liver, and kidney were isolated from either PBS- or M/CpG-ODN-TRP2-Lipo-treated mice, prepared into Formalin-fixed, paraffin-embedded sections, and stained with hematoxylin and eosin.

The vascular density within the tumor tissue was examined by immunohistochemistry (IHC) using anti-CD31 antibody. The proliferative activity of the tumor was evaluated using anti-PCNA antibody. Apoptosis within the tumor tissue was detected by the terminal deoxynucleotidyl transferase dUTP nick end labeling (TUNEL) assay according to the *In Situ* Cell Death Detection Kit-Fluorescein manual (Roche Diagnostics, Hoffman-La Roche, Basel, Switzerland). For every tumor section, five random images were taken. The positive signals were analyzed and quantified using Image-Pro Plus 5.0 software (Media Cybernetics, Warrendale, PA, USA).

In situ tetramer analysis for TRP2-specific CD8+ T cells within the tumor

Frozen sections (8 µm thick) of tumor tissues were prepared. After being blocked in rat serum, the sections were incubated with TRP2 tetramer (conjugated to PE) and anti-CD8 antibody (conjugated to FITC) at 37°C for 30 min. After three washes with PBS, the sections were stained with DAPI for 30 min and imaged under fluorescence microscopy.

Statistical analysis

The statistical analysis was performed using SPSS16.0 software (SPSS Inc., Chicago, IL, USA). Each datum represents the mean ± SD of at least three independent experiments. Differences among groups were compared by two-tailed *student's t*-test and ANOVA. Mouse survival time was analyzed using the Kaplan-Meier method and differences between each group were studied by the log-rank test. A *p* value of < 0.05 was considered statistically significant. In the figures, * denotes $p < 0.05$, ** denotes $p < 0.01$, and *** denotes $p < 0.001$.

Results

Physical characterization of liposomal particles

A schematic diagram for the preparation and function of M/CpG-ODN-TRP2-Lipo particles is shown in Figure 1. The synthesis results of mannose lipid were analyzed by FTIR. As shown in Figure S1A, mannose lipid presented absorption peaks at 3328 cm⁻¹, 2918 cm⁻¹, and 1703 cm⁻¹, consistent with the composing –OH, –CH3 and –CH2, and –C=O groups, respectively. As a comparison, palmic acids exhibited absorption peaks at 2918 cm⁻¹ and 1703 cm⁻¹; and mannose exhibited absorption peaks at 3285 cm⁻¹ and 1629 cm⁻¹, respectively. Consistently, the XRD analysis of the synthesized mannose lipid (as shown in Figure S1B) revealed strong absorption peaks at $2\theta = 21.3°$, 23.8°, and 28.9°, which were different from those for palmic acid ($2\theta = 21.2°$, 22.7°, 24.3°, and 26.1°) and mannose ($2\theta = 21.4°$ and 24.0°; Figure 1B). The morphological structure and size of the three liposomes were determined by TEM. As shown in Figure 2, all liposomal complexes presented as uniform spheres of similar particle diameters upon hydration (~100 nm for both M/CpG-ODN-TRP2-Lipo and M/CpG-ODN-Mut1-Lipo and 127 nm for M/CpG-ODN-B16-Lipo). The particle size, zeta potential, and PDI of all three liposomes as measured by the Zetasizer are listed in Table 1. All three liposomes were negatively charged. The encapsulation rate of the antigens for M/CpG-ODN-TRP2-Lipo, M/CpG-ODN-Mut1-Lipo and M/CpG-ODN-B16-Lipo were 60.8%, 62.7%, and 48.9%, respectively.

Table 1. Particle size, polydispersity index (PDI), and zeta potential of the liposomes.

Liposome type	Particle size (nm, ± SD)	PDI (± SD)	Zeta Potential (mV, ± SD)
M/CpG-ODN-Mut1-Lipo	103 ± 7	0.132 ± 0.012	-7.7 ± 0.5
M/CpG-ODN-B16-Lipo	127 ± 6	0.245 ± 0.006	-5.3 ± 0.2
M/CpG-ODN-TRP2-Lipo	102 ± 9	0.156 ± 0.022	-17.3 ± 0.5

In vitro characterization of the liposomal particles

To examine the targeting specificity of M-Lipo towards DCs, we labeled the liposome particles with the red fluorescent dye DiI and monitored their subsequent phagocytosis by DCs. As shown in Figure 3A, the liposomal particles (Lipo) failed to be effectively engulfed by the DCs. As a comparison, liposomal particles modified with mannose (M-Lipo) significantly accumulated inside the DCs. We also

performed a competitive assay to further confirm that phagocytosis is mediated by mannose. Our data revealed that pre-blocking of DCs with 0.5% mannose overnight dramatically reduced the uptake of liposomal particles (Figure 3B). Next, we assessed the linkage status of CpG-ODN to liposome particles using the FITC-labeled CpG-ODN. As shown in Figure 3C, DCs engulfing M-Lipo only showed red fluorescence, while DCs engulfing M/CpG-ODN-Lipo showed overlap of red and green fluorescence, indicating the successful conjugation of CpG-ODN to liposome particles.

To characterize cellular uptake of liposomes functionally, we examined the surface expression of DC activation markers, including MHC-II, CD80, and CD86. The expression levels of all three markers were significantly up-regulated in DCs following the stimulation of M/CpG-ODN-TRP2-Lipo compared with those of M-Lipo and M/CpG-ODN-Lipo. Also, our results evidenced that the combination of mannose and CpG-ODN (M/CpG-ODN-Lipo)

showed superior efficacy to stimulate the activation of DCs over the singular use of M-Lipo ($p < 0.05$; Figure 4).

Also, we measured the stability of M/CpG-ODN-TRP2-Lipo in serum. The data revealed that DC activation (determined by the expression of CD80 and CD86) was significantly stimulated by M/CpG-ODN-TRP2-Lipo particles, which were preserved in serum for up to 10 days ($p < 0.05$; Figure 5).

In vivo anti-melanoma activity and safety evaluation of M/CpG-ODN-TRP2-Lipo

We further assessed the *in vivo* antitumor activity of the M/CpG-ODN-TRP2-Lipo in a B16 melanoma model. B16-bearing mice were treated with PBS, M/CpG-ODN-Mut1-Lipo, M/CpG-ODN-B16-Lipo, or M/CpG-ODN-TRP2-Lipo, respectively. The differences in tumor volume of the four groups were significant by day 15 (post-injection of B16 cells) ($p < 0.01$; Figure 6B). On day 17 (post-injection of B16 cells), the tumors were isolated from the mice. Obviously, tumors from M/CpG-ODN-TRP2-
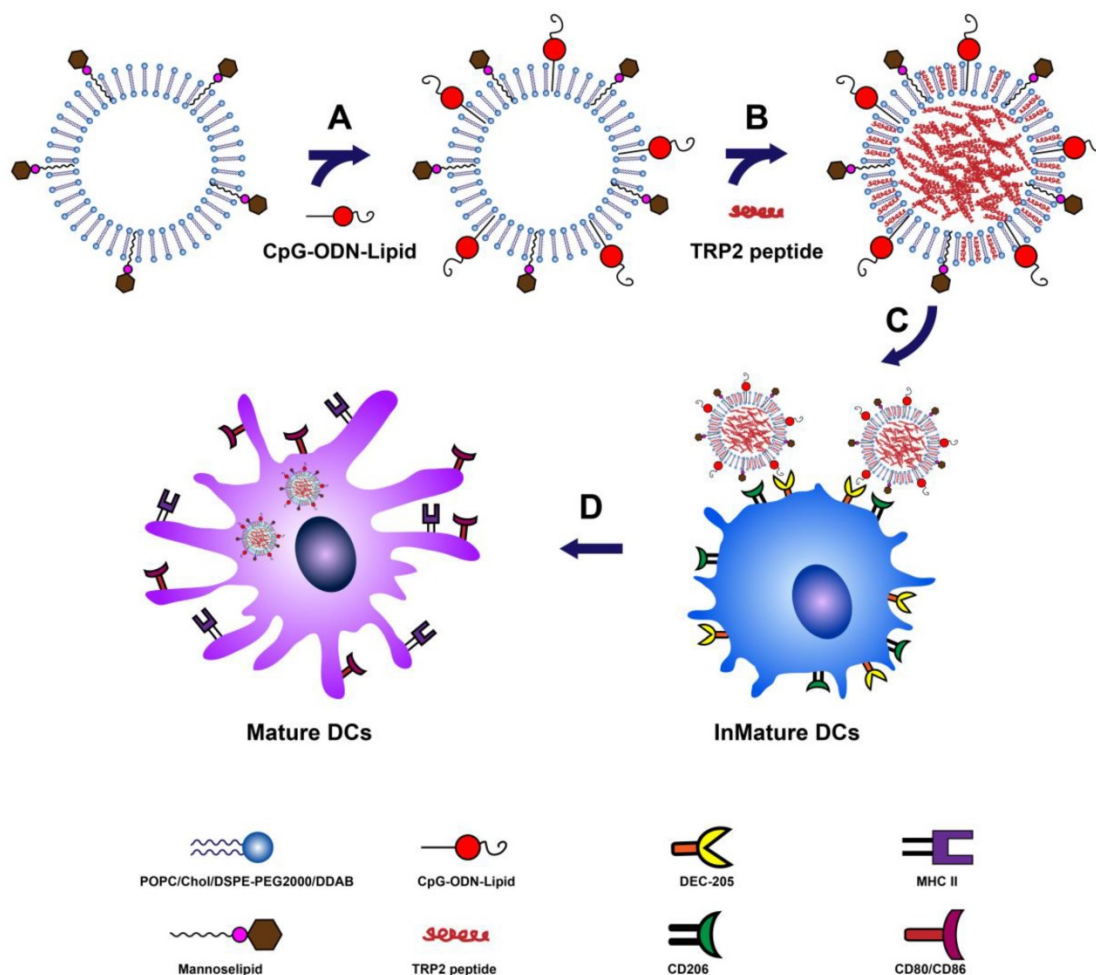

Figure 1. Schematic description of the preparation and function of M/CpG-ODN-TRP2-Lipo. (A) Conjugation of CpG-ODN to M-Lipo; (B) encapsulation of TRP2 peptide in M/CpG-ODN-Lipo; (C) binding of mannose with mannose receptors and CpG-ODNs with their cell surface receptors, such as DEC-205, on DCs; (D) after entry into DCs, M/CpG-ODN-TRP2-Lipo is delivered to the endosomes, enabling the activation and maturation of DCs.

Lipo-treated mice were much smaller than those from the other treatment groups (Figure 6A). Consistently, the survival time of the mice treated with M/CpG-ODN-TRP2-Lipo (with a median survival time of 40 days) was significantly higher than mice treated with PBS, M/CpG-ODN-Mut1-Lipo, or M/CpG-ODN-B16-Lipo (with median survival times of 22 days, 26 days, and 30 days, respectively) ($p <$ 0.01; Figure 6C). In addition, we evaluated the safety of M/CpG-ODN-TRP2-Lipo in C57BL/6 mice. All the mice were dissected 7 days after injection of M/CpG-ODN-TRP2-Lipo or PBS. The harvested tissue specimens, including lung, spleen, liver, and kidney, did not reveal any sign of infiltration of inflammatory cells (Figure 6D). These data suggested that the administration of M/CpG-ODN-TRP2-Lipo caused a significant tumor growth inhibition compared with the other therapies. At the same time, M/CpG-ODN-TRP2-Lipo treatment was relatively safe in mice.

In vivo immune regulation following the administration of M/CpG-ODN-TRP2-Lipo

To evaluate the antitumor response induced by M/CpG-ODN-TRP2-Lipo, we investigated the number of MDSCs, Tregs, activated T cells, and TRP2-specific CD8$^+$ CTLs by flow cytometry. Also, we examined the number of IFN-γ-producing cells by the ELISPOT method. Our data revealed the proportions of MDSCs (CD11b$^+$Ly6G$^+$) were dramatically reduced in tumor, marrow, and spleen of mice treated with M/CpG-ODN-TRP2-Lipo in comparison with those treated with M/CpG-ODN-Mut1-Lipo, M/CpG-ODN-B16-Lipo, or PBS, respectively ($p <$ 0.05, Figure 7A). Similarly, the proportion of CD25$^+$FoxP3$^+$ Tregs in spleen significantly decreased in mice treated with M/CpG-ODN-TRP2-Lipo compared with those receiving other therapies. ($p <$ 0.01; Figure 7B). In contrast, the number of activated T cells (CD3$^+$CD25$^+$ T cells; Figure 7C), TRP2-specific CD8$^+$ CTLs (as detected by TRP2 tetramer; Figure 7D), and IFN-γ-producing cells (Figure 7E) in spleen significantly increased in response to M/CpG-ODN-TRP2-Lipo treatment ($p <$ 0.001 vs. the other treatments). These data suggested that M/CpG-ODN-TRP2-Lipo treatment induced a systemic up-regulation of antitumor immunity and down-regulation of immunosuppression.
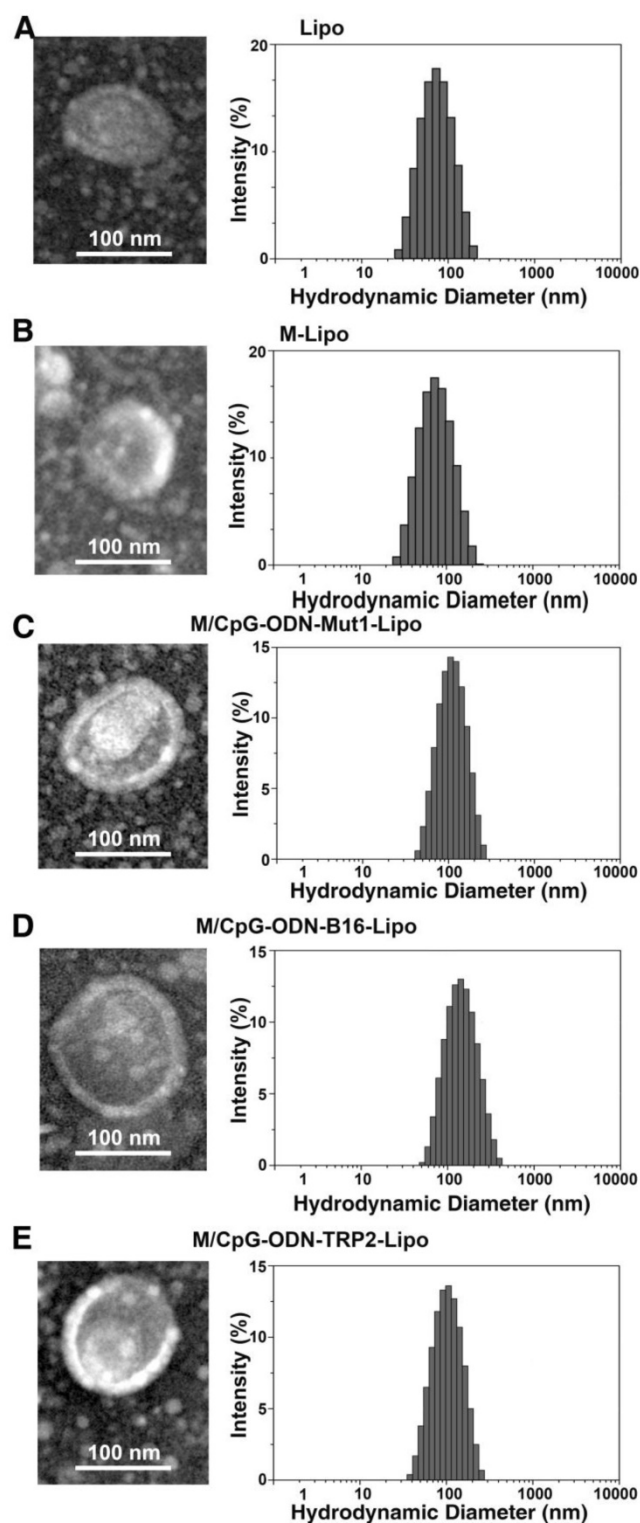

Figure 2. Characterization of the prepared liposomal particles. TEM (200,000×, left) and particle distribution as measured using a Zetasizer instrument (right). (A) Lipo; (B) M-Lipo; (C) M/CpG-ODN-Mut1-Lipo; (D) M/CpG-ODN-B16-Lipo; (E) M/CpG-ODN-TRP2-Lipo.
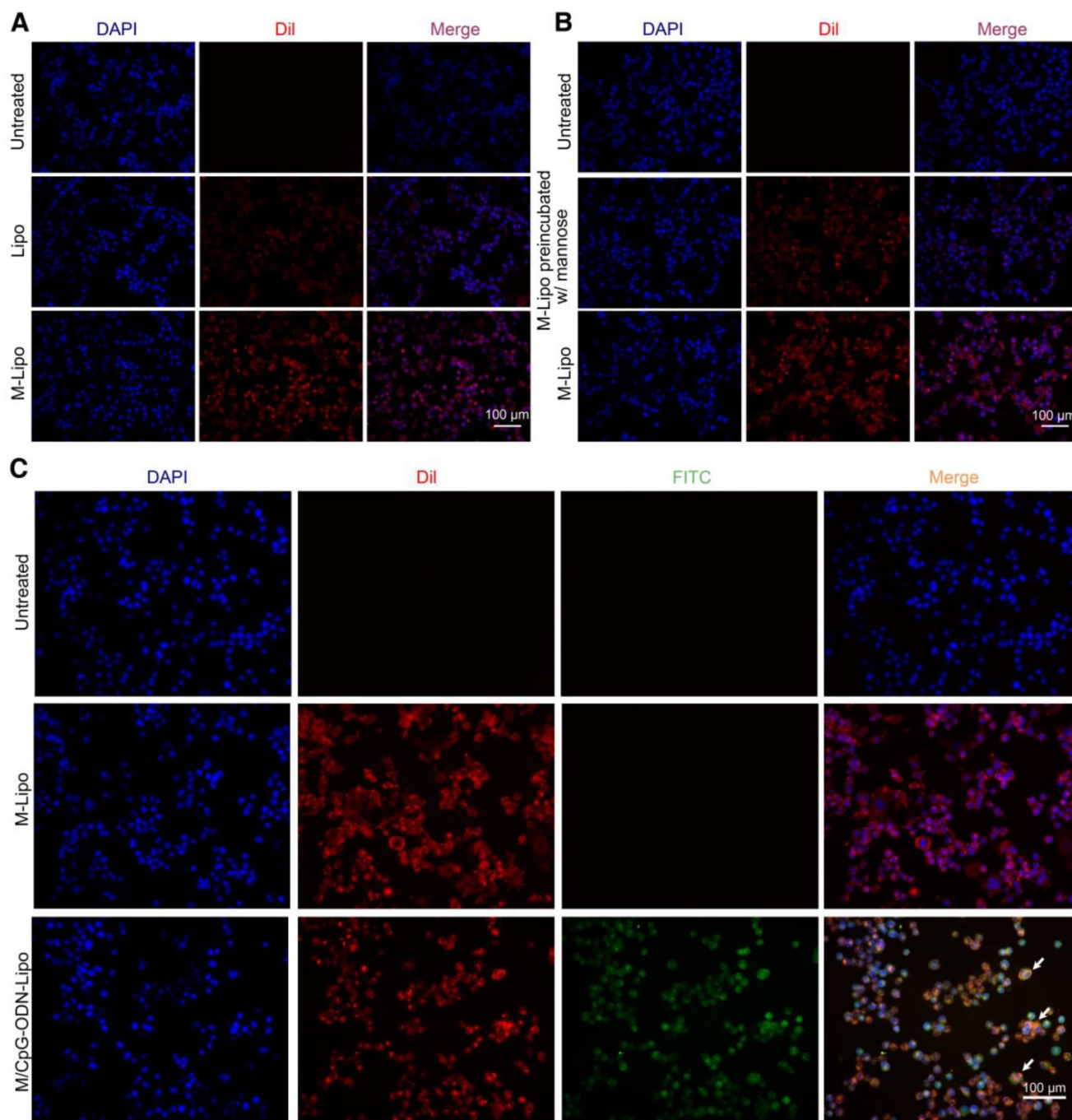
Figure 3. Uptake of liposomes in DCs. (A) DCs were treated with Lipo (middle panel) or M-Lipo (lower panel) at 37℃ for 2 h, respectively. Compared with Lipo, M-lipo particles were effectively taken up by the DCs. Untreated DCs served as a blank control. (B) Upper panel: untreated DCs; middle panel: DCs preblocked with 0.5% free mannose were treated with M-Lipo; lower panel: DCs were treated with M-Lipo. Images demosntrate that pre-incubation of DCs with 0.5% free mannose dramatically reduced the uptake of M-Lipo by DCs. Untreated DCs served as a blank control. (C) DCs were treated with M-Lipo (middle panel) or M/CpG-ODN-Lipo (lower panel) at 37℃ for 2 h, respectively. Untreated DCs served as a blank control. Images demonstrate that liposomal particles modified either with mannose alone or both mannose and CpG-ODN were effectively taken up by the DCs. Arrows indicate DCs engulfing liposomal particles modified with both CpG-ODN and mannose. Red signal, Dil-labeled mannose lipid; blue signal, DAPI nuclear stain; green signal, FITC–labeled CpG-ODN. Magnification, 200×.

Treatment with M/CpG-ODN-TRP2-Lipo significantly inhibited tumor angiogenesis and proliferation, while promoting tumor apoptosis in mice

We also examined tumor angiogenesis, tumor cell proliferation and apoptosis in response to M/CpG-ODN-TRP2-Lipo therapy. Immunohisto-chemical analysis by CD31 (vascular endothelial marker) and PCNA (proliferation marker) staining showed that angiogenesis and the number of PCNA+ proliferative cells were significantly reduced when mice were treated with M/CpG-ODN-TRP2-Lipo ($p <$ 0.001 compared to PBS, M/CpG-ODN-Mut1-Lipo, or

M/CpG-ODN-B16-Lipo treatment group; Figure 8). Similarly, the TUNEL assay revealed that M/CpG-ODN-TRP2-Lipo therapy caused a significant increase in the number of apoptotic cells in tumor tissues as compared to all other treatment groups ($p < 0.001$; Figure 8).
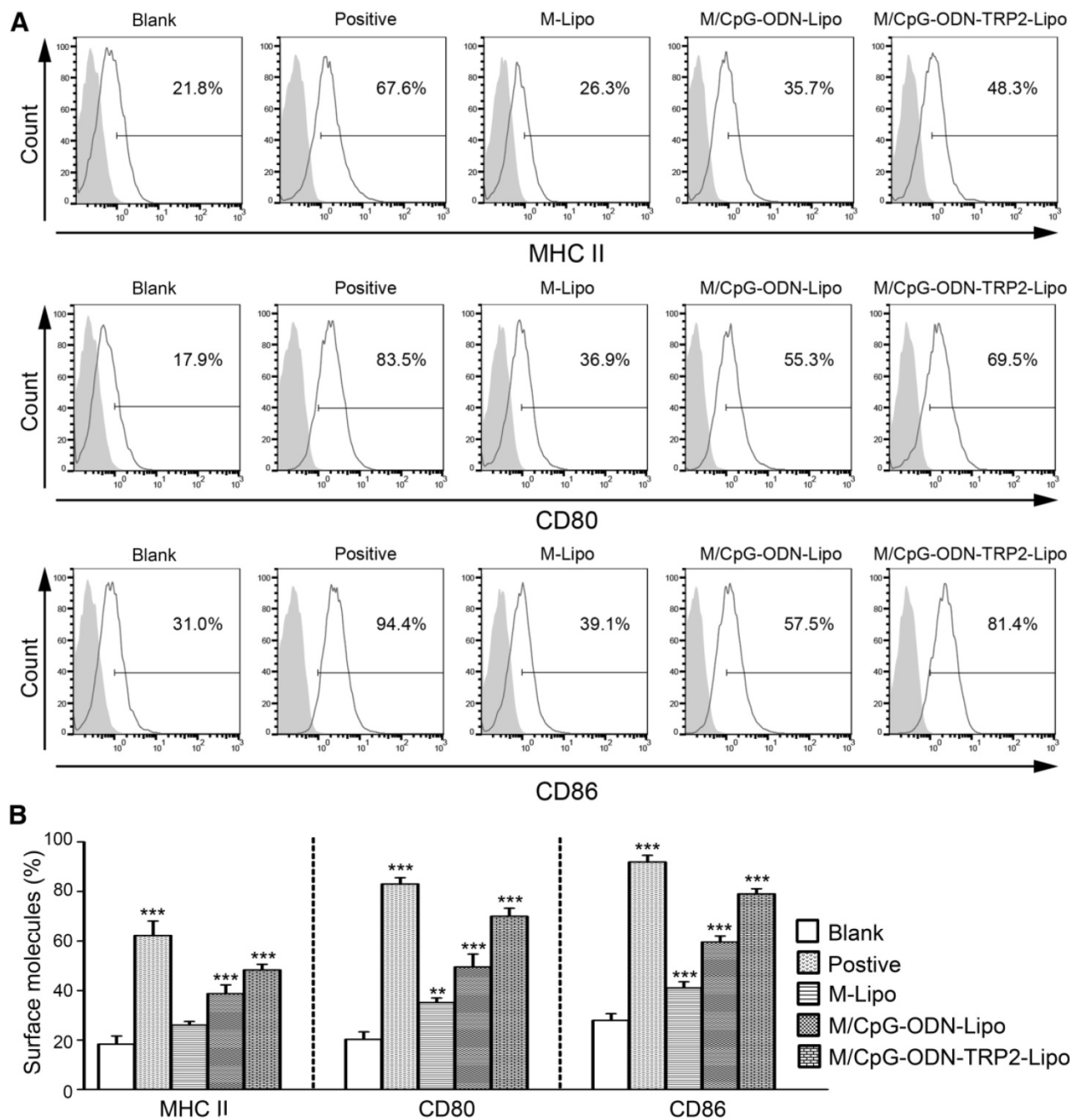

Figure 4. M/CpG-ODN-TRP2-Lipo treatment induced higher levels of MHC II, CD80, and CD86. (A) The levels of MHC II, CD80 and CD86 expression were measured by flow cytometry. (B) Quantitative analysis. Data are expressed as mean ± SD of each group (n = 3). Untreated DCs served as a blank control. DCs treated with TNF-α served as a positive control. * $p < 0.05$, ** $p < 0.01$, *** $p < 0.001$.
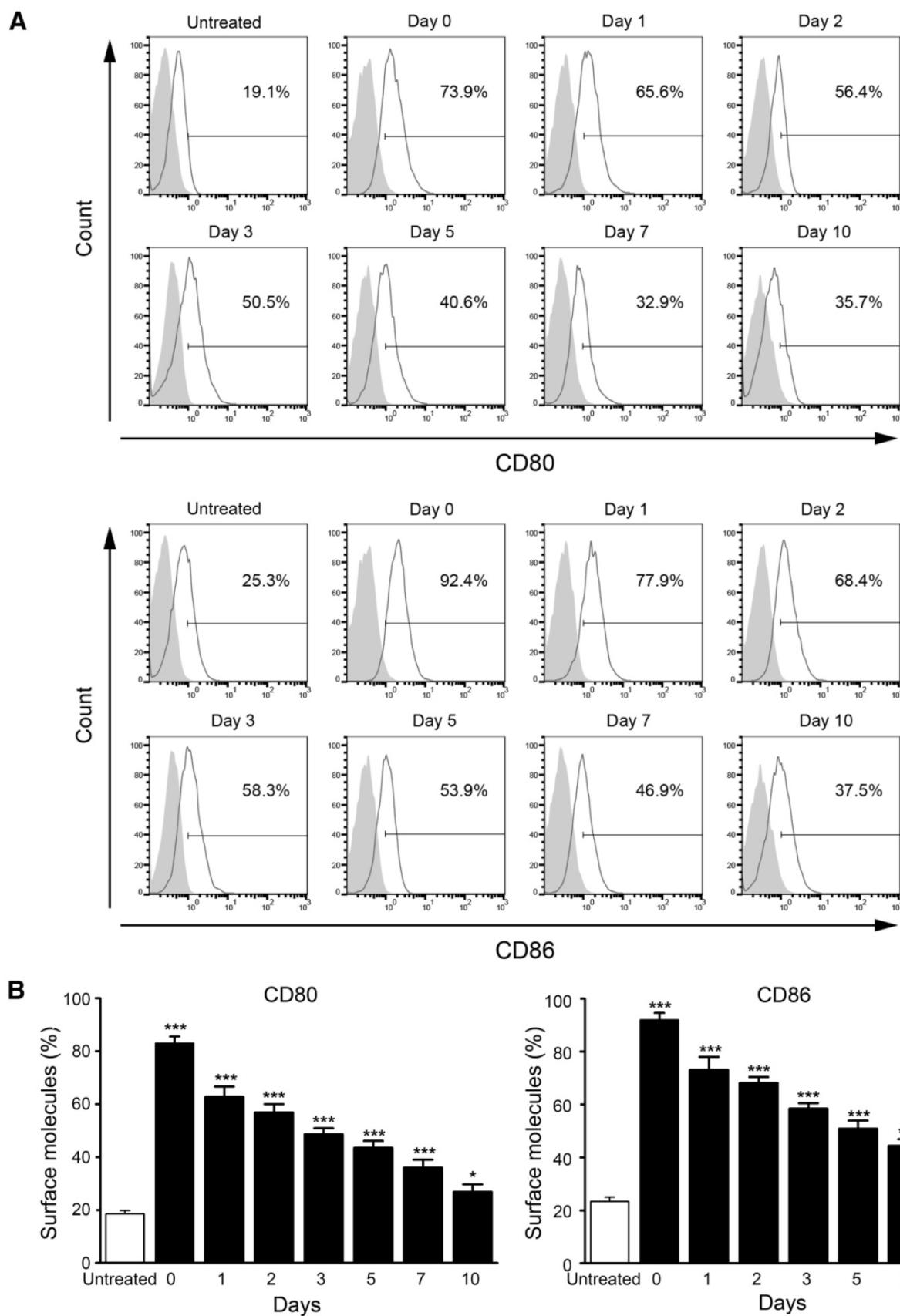
Figure 5. Stability analysis of M/CpG-ODN-TRP2-Lipo particles in serum. (A) The levels of CD80 and CD86 expression were measured by flow cytometry. (B) Quantitative analysis. Data are presented as mean ± SD of each group (n = 3). Untreated DCs served as a blank control. * $p < 0.05$, ** $p < 0.01$, *** $p < 0.001$ vs. the untreated samples.
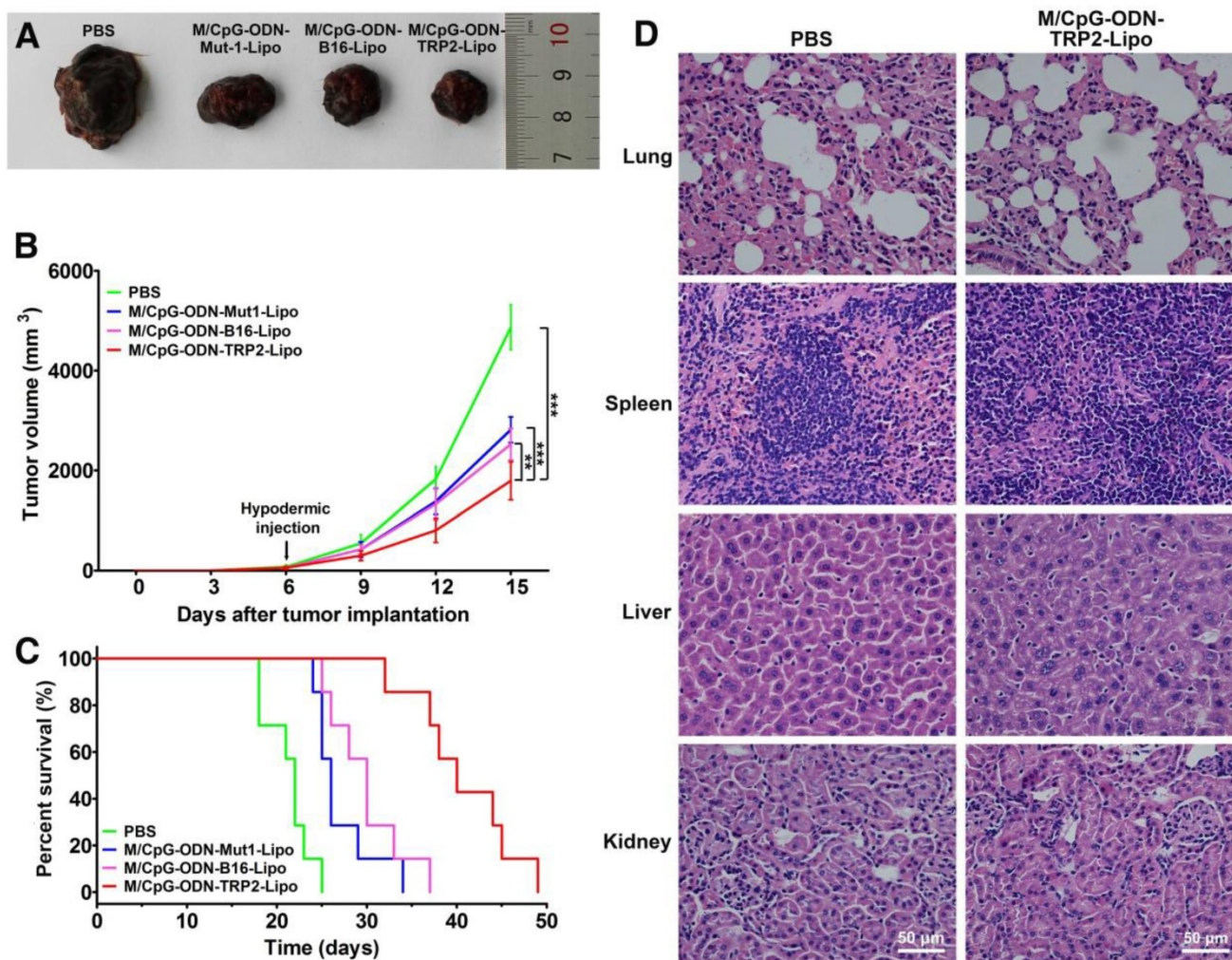
Figure 6. Effects of the treatment of B16-bearing mice with the liposomal particles and safety evaluation of the M/CpG-ODN-TRP2-Lipo particles. (A) Photographs of tumors from each treatment group; (B) tumor volumes. Data are expressed as mean ± SD of the tumor volumes of each group (n = 8 mice per group). ** $p < 0.01$, *** $p < 0.001$. (C) Survival analysis. Treatment with M/CpG-ODN-TRP2-Lipo significantly enhanced survival, as compared with treatment with M/CpG-ODN-Mut1-Lipo, M/CpG-ODN-B16-Lipo or PBS, respectively (n = 8 mice per group, $p < 0.01$). Median survival in days for each treatment group: PBS treatment, 22 d; M/CpG-ODN-Mut1-Lipo treatment, 26 d; M/CpG-ODN-B16-Lipo treatment, 30 d; M/CpG-ODN-TRP2-Lipo treatment, 40 d. (D) Safety evaluation of the M/CpG-ODN-TRP2-Lipo. Representative images (400×) of lung, spleen, liver, and kidney tissue sections from mice treated with either PBS or M/CpG-ODN-TRP2-Lipo were stained with H&E.

Tumor-specific CD8+ CTL induced by M/CpG-ODN-TRP2-Lipo therapy

To analyze whether the decrease in angiogenesis and tumor cell proliferation and the increase in apoptosis were associated with local immune alterations in the tumor tissue, we explored the presence of TRP2-specific CD8+ CTLs in tumor of each group. As shown in Figure 9, although the infiltration of CD8+ T cells was detected in the tumor tissues from all four groups, the TRP2-specific CD8+ cells were only detected in the tumor tissues harvested from the M/CpG-ODN-TRP2-Lipo-treated group. These data suggested that the M/CpG-ODN-TRP2-Lipo therapy induced a tumor-specific CD8+ CTL response.

Antitumor activity of M/CpG-ODN-TRP2-Lipo was affected by loss of MyD88

The myeloid differentiation primary response gene 88 (MyD88) is a critical regulator of Toll-like receptor (TLR)-mediated immune signaling in dendritic cells [34]. To examine whether the MyD88 pathway might play a role in M/CpG-ODN-TRP2-Lipo therapy, we established the melanoma models of B16 cell line in Myd88-knockout mice. Our data revealed that MyD88 knockout mice had significantly shorter median survival times (with a median survival time of 30 days) compared to wild-type mice (with a median survival time of 40 days) following the administration of M/CpG-ODN-TRP2-Lipo ($p < 0.01$; Figure 10).
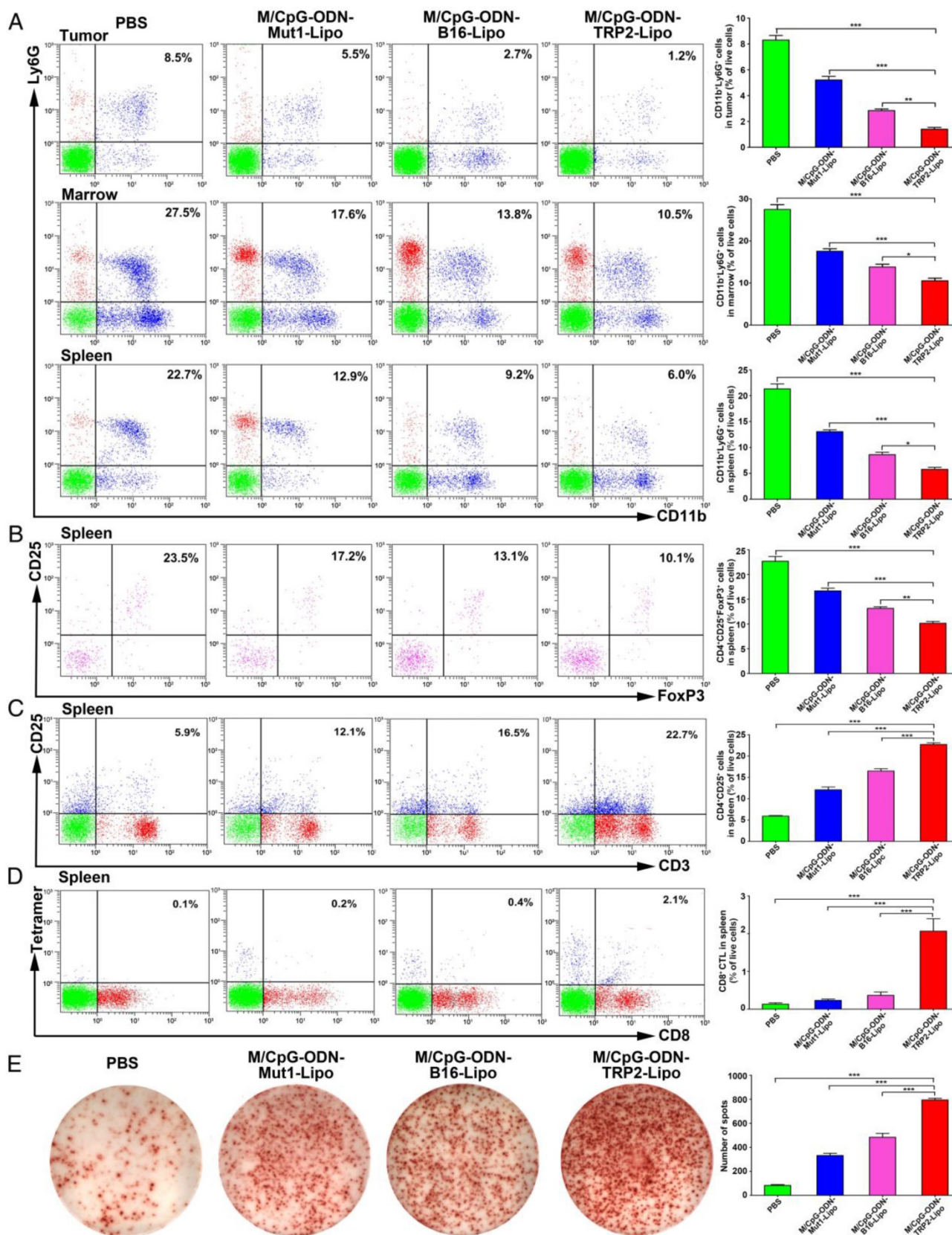
Figure 7. Effects of the treatment of B16-bearing mice with the liposomal particles. The frequencies of CD11b+Ly6G+ MDSCs (in the tumor, marrow, and spleen), CD25+FoxP3+ Tregs (in the spleen), CD3+CD25+ activated T cells (in the spleen), and TRP2-specific CD8+ cells (in the spleen) were determined by flow cytometry. IFN-γ-producing cells in the spleen were detected by ELISPOT assay. (A-D) Flow cytometry analysis of MDSCs, Tregs, activated T cells, and TRP2-specific CD8+ cells. Data are presented as representative images (on the left) or expressed as mean ± SD of each group (on the right, n = 3) of cells. (E) ELISPOT analysis of the number of IFN-γ-producing cells in the spleen. Data are presented as representative images (on the left) or expressed as the mean ± SD of the number of spot-forming clones of each group of mice (on the right, n = 3). * $p < 0.05$, ** $p < 0.01$, *** $p < 0.001$.
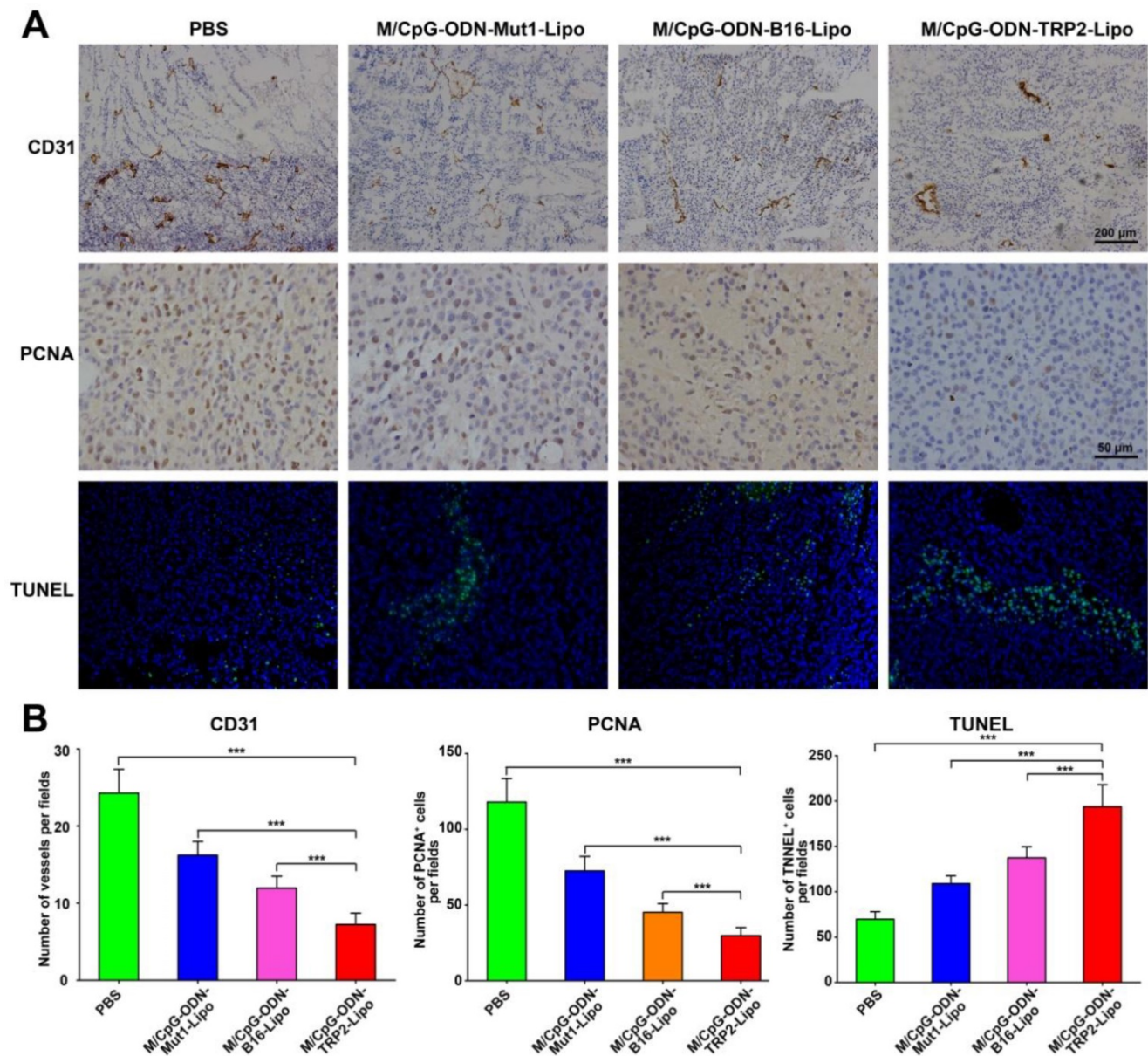
Figure 8. Effects of the treatment of B16-bearing mice with the liposomal particles. (A) Visualization of angiogenesis and cell proliferation in tumor tissue sections from mice in each treatment group by immunohistochemical staining with anti-CD31 antibody (100×, the upper panel) or anti-PCNA antibody (400×, the middle panel), respectively. Visualization of cell apoptosis in tumor tissue sections from mice in each treatment group by TUNEL (200×, the lower panel). (B) Quantitative analysis. Data are presented as the mean ± SD of each group of tumors, n = 5, *** $p < 0.001$.

Discussion

Here we reported a novel liposomal vaccine, M/CpG-ODN-TRP2-Lipo, which contained both lipid-CpG-ODN and lipid-mannose conjugates, as DC-targeting carrier for TRP2$_{180-188}$, a melanoma-specific antigen peptide. FTIR, X-ray diffractometry, particle size distribution, TEM and zeta potential analysis confirmed the successful synthesis of M/CpG-ODN-TRP2-Lipo nanoparticles. We demonstrated *in vitro* that the prepared particles were efficiently taken up by DCs. We found that the uptake led to enhanced activation of DCs, as

evidenced by the upregulation of MHC, CD80 and CD86 molecules. DCs are antigen presenting cells capable of intaking and processing antigens and present the antigen peptide complex to CD4$^+$ T cells (Helper T cells, Th) by the classical antigen presentation pathway forming MHC II–peptide complex. Addionally, they also present the antigen peptide complex to CD8$^+$ T cells (cytotoxic T lymphocyte, CTL) by the cross presentation pathway forming MHC I–peptide complex [35-36]. M/CpG-ODN-TRP2-Lipo may also be able to activate T cells by cross-presentation, thus achieving antitumor effect. The liposomal vaccine effectively inhibited tumor growth and prolonged the survival of

tumor-bearing mice. It significantly reduced the number of MDSCs and Tregs, while simultaneously increasing the number of activated T cells, tumor antigen-specific CD8+ CTLs, and IFN-γ-producing cells, thus inducing an effective cellular immune response. The liposomal vaccine significantly inhibited tumor angiogenesis and tumor cell proliferation while promoting their apoptosis. Collectively, our results indicate the potential of this liposomal vaccine for the treatment of melanoma in the clinic.

CpG-ODNs have potent immunostimulatory properties and are being used in many clinical vaccine trials implemented to verify their effects [37-39]. Recently, it was reported that lipid-conjugated CpG-ODNs, an alternative to encapsulation inside liposomes, can be used to enhance the delivery of CpG-ODNs to TLR9 in the endosome [40, 41]. In this report, we describe the CpG-ODN molecules conjugated on the liposome surface as a means to exert their immunostimulatory capabilities. Yet,

simply adding CpG-ODNs to the vaccine may fail to reduce or reverse the growth of established tumors. Combination strategies may be the key to the success of DC-based cancer vaccines. It was reported that α-D-mannose or mannoproteins synergized with CpG-ODNs had the potential to enhance immune responses [42-45]. Co-delivering synergistic DNA CpG, RNA, and peptide into antigen presenting cells (APCs) are innovative methods in cancer immunotherapy [46]. Mannosylated cationic liposomes/immunostimulatory CpG DNA complex induced a higher TNF-alpha production in contrast to the CpG DNA complexed with conventional cationic liposomes and galactosylated cationic liposomes [47]. Based on this rationale, we conjugated both CpG-ODN and mannose on the surface of the liposomal vaccine. Consequently, our flow cytometry data demonstrated that the activation of DCs was significantly promoted after the cells were cooperatively stimulated by CpG-ODN and mannose molecules.
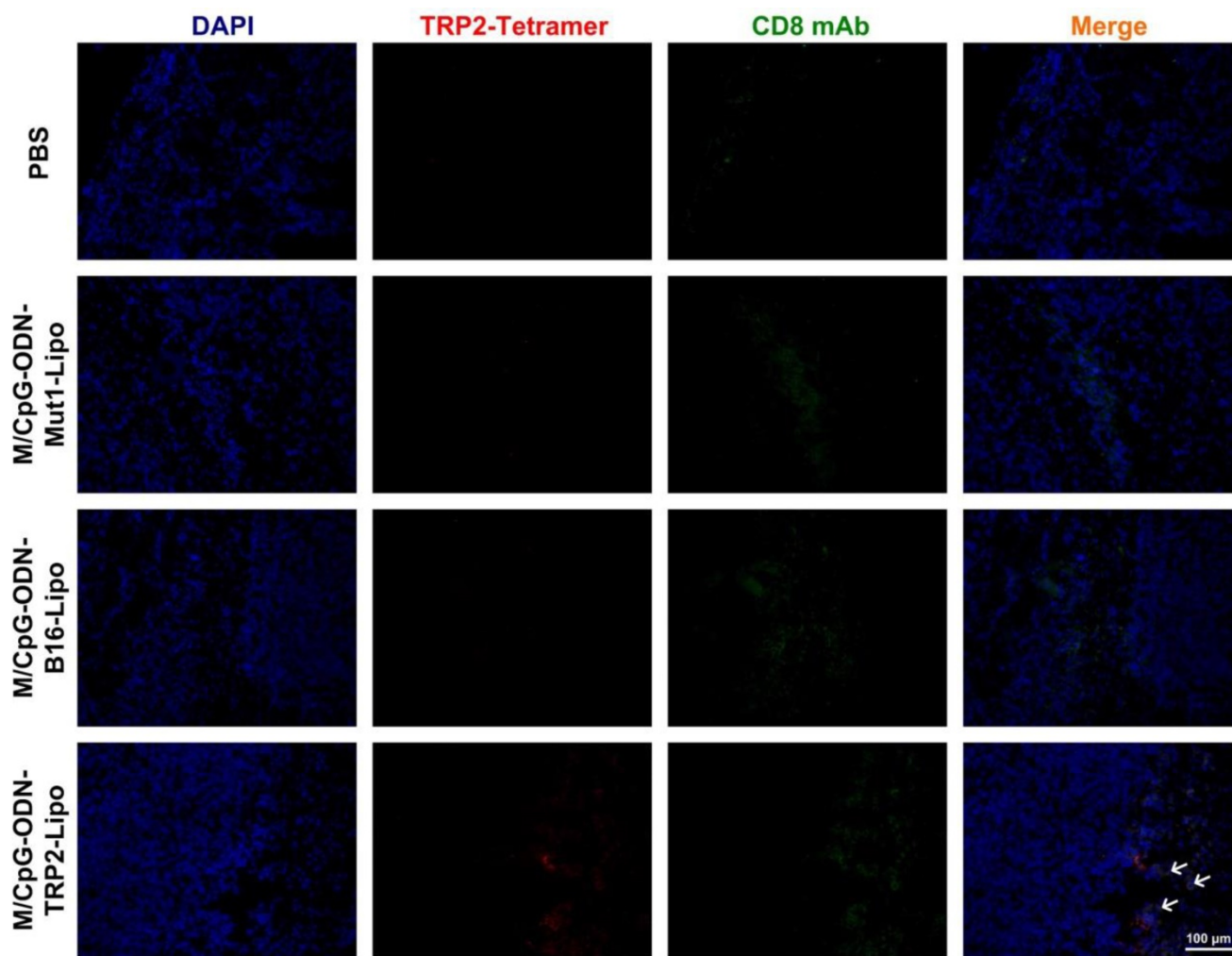

Figure 9. Effects of treatment of B16-bearing mice with the liposomal particles. Tumor tissue sections were stained with TRP2-tetramer and anti-CD8 antibody. Red signal: phycoerythrin-labeled TRP2-tetramer stain; green,signal: FITC-labeled anti-CD8 antibody; blue, signal: 4',6-diamidino-2-phenylindole nuclear stain. Magnification, 200×. Arrows indicate TRP2-specific CD8+ CTLs.
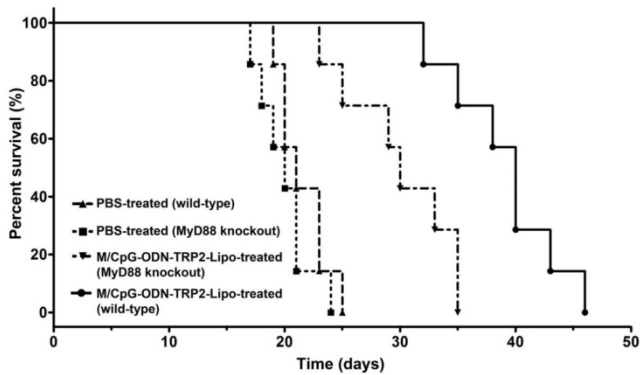
Figure 10. Antitumor activity of M/CpG-ODN-TRP2-Lipo was affected by loss of MyD88. Wild-type or MyD88 knockout B16-bearing mice were treated with PBS or M/CpG-ODN-TRP2-Lipo, respectively. Mice were monitored for survival (n = 7 mice per group). Survival data are plotted as a Kaplan-Meier curve. Median survival in days for each group: PBS-treated wild-type mice, 21 d; PBS-treated MyD88 knockout mice, 20 d; M/CpG-ODN-TRP2-Lipo-treated wild-type mice, 40 d; M/CpG-ODN-TRP2-Lipo-treated MyD88 knockout mice, 30 d. MyD88 knockout mice had significantly shorter median survival times compared to wild-type mice following the administration of M/CpG-ODN-TRP2-Lipo. ** $p < 0.01$.

Additionally, our data revealed that the Myd88-knockout mice treated with M/CpG-ODN-TRP2-Lipo had a much shorter survival time as compared to that of the wild-type mice. These results suggested that the antitumor activities of this liposomal vaccine, containing CpG-ODN, partially rely on the Myd88 signaling pathway. The results extended the previous observation that CpG-OND molecules initiate cellular signaling by triggering TIR-TIR homophilic interaction with TIR domain-containing TLR adaptors, such as myeloid differentiation primary response protein 88 (MyD88, one of the most common TLR adaptors) [48, 49].

Dendritic cell (DC)-based vaccines encapsulating either whole tumor cell lysates or short synthetic peptides within the defined tumor associated antigens (TAAs) have been widely used in research and clinical applications. However, comparisons of their feasibility and antitumor effect have never been reported. In the present study, *in vivo* antitumor effects and antitumor immune responses induced by the delivery of melanoma-specific antigen peptides (TRP2$_{180-188}$) or B16 melanoma whole-cell lysates towards DCs were explored parallelly for the first time. We found that, compared to the total tumor-cell lysate-based vaccine (M/CpG-ODN-B16-Lipo), the tumor-specific antigen peptide-based vaccine (M/CpG-ODN-TRP2-Lipo) induced stronger antitumor effects, accompanied by enhanced antitumor immune responses. Although cell lysates from B16 melanoma theoretically contain a whole array of TAAs that helps to generate strong overall antitumor response, the presence of non-antigenic

proteins may compete for encapsulation into the liposomal carriers and/or presentation by DCs to T cells, thus limiting their abilities to stimulate a robust immune response.

Myeloid-derived suppressor cells (MDSCs) and CD25+FoxP3+ Treg cells are major components of the immune-suppressive tumor microenviroment, the reversal of which is one of the major current challenges to immune therapy [50]. High frequency of MDSCs or Tregs is a key feature of immune suppression with strong inhibition and dysfunction of activated T cells and CD8+ cytotoxic T lymphocytes. In contrast, decreased numbers of MDSCs and Tregs are associated with a reduction in tumor volume in cancer patients [51]. Our data demonstrated that the liposomal vaccine effectively reduced the number of MDSCs and Tregs while increasing the number of activated T cells, tumor antigen-specific CTLs, and IFN-γ-producing cells. The MHC-tetramer technology allows detecting and enumerating specific T-cells targeting to tumor antigens, with exceptional sensitivity and specificity [52]. In this study, our tetramer-based flow cytometry data clearly demonstrated that administration of M/CpG-ODN-TRP2-Lipo substantially increased the TRP2-specific CD8+ CTLs in the spleen of tumor-bearing mice. Additionally, *in situ* tetramer-based staining visualized the accumulation of TRP2-tetramer+CD8+ CTLs in the tumor tissue in response to the therapeutic vaccine. The results indicate the potential for M/CpG-ODN-TRP2-Lipo to enhance the antitumor effects by alleviating the immunosuppressive environment in tumors.

In summary, our results demonstrated that M/CpG-ODN-TRP2-Lipo efficiently enhanced anti-melanoma effects in mice by alleviating immune suppression. Although the treatment efficacy of the liposomal particles is somewhat limited, it significantly prohibited tumor cell proliferation and triggered their apoptosis, thus inhibiting tumor growth and prolonging the survival of tumor-bearing mice. Interestingly, our results evidenced that combinations of immunostimulatory molecules, such as mannose and CpG-ODN, showed superior efficacy to stimulate the activation of DCs over their singular use, suggesting that seeking optimal combinations of adjuvants may provide a better chance in the development of novel DC-based vaccines. Additionally, we described that tumor-specific antigen peptide-based cancer vaccine induced stronger antitumor effects than that of the whole tumor cell lysate-based vaccine. Recently, it was reported that CpG-ODN mixed with incomplete Freund's adjuvant (IFA), a non-specific tumor vaccine adjuvant, promoted a rapid and strong human CD8+

T-cell response to vaccination [53]. We believe that comparisons of M/CpG-ODN-TRP2-Lipo vaccine with IFA/CpG are worthy of further exploration. Accordingly, we will further make comparison for the present vaccine formulation (M/CpG-ODN-TRP2-Lipo) with IFA/CpG in the near future. Overall, the liposomal vaccine, M/CpG-ODN-TRP2-Lipo, may have potential clinical value for the treatment of melanoma. In recent years, numerous clinical studies exploring the application of DC-based vaccine in combination with traditional and experimental agents have been driving a resurgence of interest; our lab is considering the best practices for different therapy combination strategies to move the therapeutics from the bench to the bedside.

Abbreviations

DCs: dendritic cells; CpG-ODN: CpG-oligo-deoxynucleotide; TRP2: tyrosinase-related protein-2; MDSCs: myeloid-derived suppressor cells; Tregs: regulatory T cells; CTLs: cytotoxic T lymphocytes; TLR9: Toll-like receptor 9; POPC: 1-palmitoyl, 2-oleoyl-sn-glycero-3-phosphocholine; DSPE-PEG$_{2000}$: 1,2-distearoyl-sn-glycero-3-phosphoethanolamine-N-[polyethylene glycol-2000]; DDAB: didecyldime-thylammonium bromide; FITC: fluorescein isothiocyanate; DAPI: 4′, 6-diamidino-2-phenylindole; PCNA: proliferating cell nuclear antigen; FTIR: fourier transform infrared spectroscopy; XRD: X-ray diffractometry; EE: encapsulation efficiency; PDI: polydispersity index; TEM: transmission electron microscopy; IFN-γ: interferon-γ; ELISPOT: enzyme-linked immunospot; IHC: immunohis-tochemistry; TUNEL: terminal deoxynucleotidyl transferase dUTP nick end labeling; MyD88: myeloid differentiation primary response gene 88; TAAs: tumor associated antigens; IFA: incomplete Freund's adjuvant.

Acknowledgments

Supplementary Material

Supplementary Figure S1.
http://www.thno.org/v08p1723s1.pdf

Competing Interests

The authors have declared that no competing interest exists.

References

1. Hanahan D, Weinberg RA. Hallmarks of cancer: the next generation. Cell. 2011; 144:646-74.
2. Coley WB. The treatment of malignant tumors by repeated inoculations of erysipelas. With a report of ten original cases. 1893. Clin Orthop Relat Res. 1991; 262:3-11.
3. Mellman I, Coukos G, Dranoff G, et al. Cancer immunotherapy comes of age. Nature. 2011; 480:480-9.
4. Dougan M, Dranoff G. Immune therapy for cancer. Annu Rev Immunol. 2009; 27:83-117.
5. Palucka K, Banchereau J. Cancer immunotherapy via dendritic cells. Nat Rev Cancer. 2012; 12:265-77.
6. Jin H, Qian Y, Dai Y, et al. Magnetic Enrichment of Dendritic Cell Vaccine in Lymph Node with Fluorescent-Magnetic Nanoparticles Enhanced Cancer Immunotherapy. Theranostics. 2016; 6:2000-14.
7. Albert ML, Pearce SF, Francisco LM, et al. Immature dendritic cells phagocytose apoptotic cells via alphavbeta5 and CD36, and cross-present antigens to cytotoxic T lymphocytes. J Exp Med. 1998; 188:1359-68.
8. Xue T, Liu P, Zhou Y, et al. Interleukin-6 Induced "Acute" Phenotypic Microenvironment Promotes Th1 antitumor Immunity in Cryo-Thermal Therapy Revealed By Shotgun and Parallel Reaction Monitoring Proteomics. Theranostics. 2016; 6:773-94.
9. Steinman RM. Decisions about dendritic cells: past, present, and future. Annu Rev Immunol. 2012; 30:1-22.
10. Steinman RM, Banchereau J. Taking dendritic cells into medicine. Nature. 2007; 449:419-26.
11. Cochran AJ, Morton DL, Stern S, et al. Sentinel lymph nodes show profound downregulation of antigen-presenting cells of the paracortex: implications for tumor biology and treatment. Mod Pathol. 2001; 14:604-8.
12. Shields JD, Kourtis IC, Tomei AA, et al. Induction of lymphoidlike stroma and immune escape by tumors that express the chemokine CCL21. Science. 2010; 328:749-52.
13. Ahmed MS, Bae YS. Dendritic cell-based therapeutic cancer vaccines: past, present and future. Clin Exp Vaccine Res. 2014; 3:113-6.
14. Gao L, Zhang C, Gao D, et al. Enhanced antitumor Efficacy through a Combination of Integrin αvβ6-Targeted Photodynamic Therapy and Immune Checkpoint Inhibition. Theranostics. 2016; 6:627-37.
15. Tacken PJ, de Vries IJ, Torensma R, et al. Dendritic-cell immunotherapy: from ex vivo loading to in vivo targeting. Nat Rev Immunol. 2007; 7:790-802.
16. Keler T, Ramakrishna V, Fanger MW. Mannose receptor-targeted vaccines. Expert Opin Biol Ther. 2004; 4:1953-62.
17. He LZ, Crocker A, Lee J, et al. Antigenic targeting of the human mannose receptor induces tumor immunity. J Immunol. 2007;: 1786259-67.
18. Mahnke K, Guo M, Lee S, et al. The dendritic cell receptor for endocytosis, DEC-205, can recycle and enhance antigen presentation via major histocompatibility complex class II-positive lysosomal compartments. J Cell Biol. 2000; 151:673-84.
19. Bonifaz LC, Bonnyay DP, Charalambous A, et al. In vivo targeting of antigens to maturing dendritic cells via the DEC-205 receptor improves T cell vaccination. J Exp Med. 2004; 199:815-24.
20. Geijtenbeek TB, Torensma R, van Vliet SJ, et al. Identification of DC-SIGN, a novel dendritic cell-specific ICAM-3 receptor that supports primary immune responses. Cell. 2000; 100:575-85.
21. Bonifaz L, Bonnyay D, Mahnke K, et al. Efficient targeting of protein antigen to the dendritic cell receptor DEC-205 in the steady state leads to antigen presentation on major histocompatibility complex class I products and peripheral CD8+ T cell tolerance. J Exp Med. 2002; 196:1627-38.
22. Hawiger D, Inaba K, Dorsett Y, et al. Dendritic cells induce peripheral T cell unresponsiveness under steady state conditions in vivo. J Exp Med. 2001; 194:769-79.
23. Van Broekhoven CL, Parish CR, Demangel C, et al. Targeting dendritic cells with antigen-containing liposomes: a highly effective procedure for induction of antitumor immunity and for tumor immunotherapy. Cancer Res. 2004; 64:4357-65.
24. Jahrsdorfer B, Weiner GJ. CpG oligodeoxynucleotides as immunotherapy in cancer. Update Cancer Ther. 2008; 3:27-32.
25. Lahoud MH, Ahmet F, Zhang JG, et al. DEC-205 is a cell surface receptor for CpG oligonucleotides. Proc Natl Acad Sci U S A. 2012; 109:16270-5.
26. Xing H, Hwang K, Lu Y. Recent Developments of Liposomes as Nanocarriers for Theranostic Applications. Theranostics. 2016; 15;6:1336-52.
27. Rosenberg SA. IL-2: the first effective immunotherapy for human cancer. J Immunol. 2014; 192:5451-8.
28. Chengcheng Z, Zhengxing Z, Kuo-Shyan L, et al. Preclinical Melanoma Imaging with 68Ga-Labeled α-Melanocyte-Stimulating Hormone Derivatives Using PET. Theranostics. 2017; 7: 805-13.

29. Parkhurst MR, Fitzgerald EB, Southwood S, et al. Identification of a shared HLA-A*0201-restricted T-cell epitope from the melanoma antigen tyrosinase-related protein 2 (TRP2). Cancer Res. 1998; 58:4895-901.

30. Sun Y, Song M, Stevanovic S, et al. Identification of a new HLA-A(*)0201-restricted T-cell epitope from the tyrosinase-related protein 2 (TRP2) melanoma antigen. Int J Cancer. 2000; 87:399-404.

31. Vasievich EA, Ramishetti S, Zhang Y, et al. TRP2 peptide vaccine adjuvanted with (R)-DOTAP inhibits tumor growth in an advanced melanoma model. Mol Pharm. 2012; 9:261-8.

32. He J, Duan S, Yu X. Folate-modified Chitosan Nanoparticles Containing the IP-10 Gene Enhance Melanoma-specific Cytotoxic CD8(+)CD28(+) T Lymphocyte Responses. Theranostics. 2016; 6:752-61.

33. Shen Z1, Reznikoff G, Dranoff G, et al. Cloned dendritic cells can present exogenous antigens on both MHC class I and class II molecules. J Immunol. 1997; 158: 2723-30.

34. Warner N, Nunez G. MyD88: a critical adaptor protein in innate immunity signal transduction. J Immunol. 2013; 190:3-4.

35. Joffre O P, Segura E, Savina A, et al. Cross-presentation by dendritic cells. Nat ure Reviews Immunology, 2012, 12(8):557.

36. Kikete S, Chu X, Li W, et al. Endogenous and tumour-derived microRNAs regulate cross-presentation in dendritic cells and consequently cytotoxic T cell function. Cytotechnology, 2016, 68(6):2223.

37. Scheiermann J, Klinman DM. Clinical evaluation of CpG oligonucleotides as adjuvants for vaccines targeting infectious diseases and cancer. Vaccine. 2014; 32:6377-89.

38. Kortylewski M, Swiderski P, Herrmann A, et al. In vivo delivery of siRNA to immune cells by conjugation to a TLR9 agonist enhances antitumor immune responses. Nat Biotechnol. 2009; 27:925-32.

39. Bode C, Zhao G, Steinhagen F, et al. CpG DNA as a vaccine adjuvant. Expert Rev Vaccines. 2011; 10:499–511.

40. Weilhammer DR, Blanchette CD, Fischer NO, et al. The use of nanolipoprotein particles to enhance the immunostimulatory properties of innate immune agonists against lethal influenza challenge. Biomaterials. 2013; 34:10305-18.

41. Andrews CD, Provoda CJ, Ott G, et al. Conjugation of lipid and CpG-containing oligonucleotide yields an efficient method for liposome incorporation. 2011; 22:1279-86.

42. Shirota H, Klinman DM. CpG-conjugated apoptotic tumor cells elicit potent tumor-specific immunity. Cancer Immunol Immunoother. 2011; 60:659-69.

43. Tian Y, Li M, Yu C, Zhang R, et al. The novel complex combination of alum, CpG ODN and HH2 as adjuvant in cancer vaccine effectively suppresses tumor growth *in vivo*. Oncotarget. 2017; doi: 10.18632/oncotarget.17504.

44. Dan JM, Wang JP, Lee CK, et al. Cooperative stimulation of dendritic cells by Cryptococcus neoformans mannoproteins and CpG oligodeoxynucleotides. PLoS One. 2008; 3:e2046. doi: 10.1371/journal.pone.0002046.

45. Heesun J, Gyeonghui Y, Hyejung M. CpG oligonucleotide and α-d-mannose conjugate for efficient delivery into macrophages. Appl Biol Chem. 2016; 59:759-63.

46. Zhu G, Mei L, Vishwasrao HD, et al. Intertwining DNA-RNA nanocapsules loaded with tumor neoantigens as synergistic nanovaccines for cancer immunotherapy. Nat Commun. 2017; 8(1):1482.

47. Kuramoto Y, Kawakami S, Zhou S, et al. Use of mannosylated cationic liposomes/immunostimulatory CpG DNA complex for effective inhibition of peritoneal dissemination in mice. J Gene Med. 2008; 10(4):392–399.

48. Kogut MH, Iqbal M, He H, Philbin V, Kaiser P, Smith A: Expression and function of Toll-like receptors in chicken heterophils. Dev Comp Immunol. 2005; 29(9):791-807.

49. Gursel M, Gursel I. Development of CpG ODN Based Vaccine Adjuvant Formulations. Methods Mol Biol. 2016; 1404:289-98.

50. Lindau D, Gielen P, Kroesen M, et al. The immunosuppressive tumour network: myeloid-derived suppressor cells, regulatory T cells and natural killer T cells. Immunology. 2013; 138:105-15.

51. Noman MZ1, Desantis G, Janji B, et al. PD-L1 is a novel direct target of HIF-1α, and its blockade under hypoxia enhanced MDSC-mediated T cell activation. J Exp Med. 2014; 211:781-90.

52. Dolton G, Tungatt K, Lloyd A, et al. More tricks with tetramers: a practical guide to staining T cells with peptide-MHC multimers. Immunology. 2015; 146:11-22.

53. Ranocchia RP, Gorlino CV, Crespo MI, et al. Arginase- dependent suppression by CpG-ODN plus IFA- induced splenic myeloid CD11b+Gr1+ cells. Immunol Cell Biol. 2012; 90:710-21.